Florence, Italy 12-16 July 2015
ICSV22
The 22nd International Congress on Sound and Vibration

INVESTIGATION INTO THE APPLICATION OF AN ACOUSTIC METAMATERIAL FOR SOUND ATTENUATION WITH AIR-FLOW

Leonardo Weber and Luis Gomez-Agustina

London South Bank University, 103 Borough Road, London, SE1 0AA, United Kingdom
e-mail: leo@andersonacoustics.co.uk

This paper presents a practical investigation into the development and potential noise control application of an acoustic metamaterial. Acoustic Metamaterials are capable of changing the natural properties of sound, giving exposure to a new range of acoustical phenomena that have never been witnessed before, such as a negative bulk modulus and a negative mass density. The material investigated consisted of a panel structure of concatenated Helmholtz resonators with diffraction characteristics, which was incorporated into an acoustic enclosure. The design aimed to attenuate sound across a wide frequency range, while allowing air to flow through the panel. Sound insertion loss tests of the enclosure were carried out in an anechoic chamber. Airflow resistance tests were also undertaken in a controlled environment. Satisfactory sound attenuation and air flow resistance results indicated this metamaterial has the potential to be used as a noise control solution for acoustic enclosures requiring ventilation.

1. Introduction

The successful creation of Electromagnetic Metamaterials [1] [2] [3] led to research in the field of mechanical waves, for which Acoustic Metamaterials were proposed and developed. Acoustic Metamaterials introduced new attributes to the theory of sound, such as sonic waves with negative bulk modulus and mass density. Although these materials have been studied theoretically and experimentally [4] [5], practical applications for this technology seem to be moving at a slower pace [6] [7] [8] [9] [10].

It is widely known that materials found in nature are constituted of atoms, which move and interact in infinite degrees of freedom. Controlling the parameters involved is extremely challenging, especially regarding the interaction of atomic structures with electromagnetic waves, such as light. The solution to this limitation comes with the introduction of Metamaterials; artificial materials with geometries designed to have properties that cannot be found in nature and that affect electromagnetic waves in a way natural molecular arrangements cannot.

A very important notion required to understand the concept of Metamaterials is that the effects observed are not related to the materials used, but to the structure created. Metamaterials are not related to the atomic properties of materials but to the way the artificial structures are built. Many different geometries and shapes can be created for different purposes, for example metamaterials with resonant properties.

This paper presents an investigation into the practical development and application of a resonant acoustic metamaterial based on an earlier prototype developed at the Mokpo National Maritime University, in South Korea [11]. The material here presented consists of a concatenated array of Helmholtz resonators intended to attenuate sound across a wide range of frequencies while allowing air to flow through them. The proposed application for this metamaterial was to use a sample area (window) initially as part of the wall of an acoustic enclosure. The application of the window allows the enclosure to maintain its sound attenuation properties at determined frequencies, while also permitting air to flow from its interior, enabling a passive ventilation system. Sound insertion loss measurements were carried out in an anechoic chamber to determine the sound attenuation capabilities of the sample. Airflow resistance characteristics were determined using a calibrated air flow test rig.

The design could potentially be used as a noise control implementation for industrial noisy machinery, as the airflow properties could provide the necessary ventilation for operational temperatures inside the enclosure, allowing the hypothetical machine to operate normally, without the need of extra ventilation and silencing systems being installed. This solution would not only reduce installation costs, but would also lower the overall energy consumption, making it more cost-effective, sustainable and environmentally friendly.

2. Resonant Metamaterials

An analogy between a mass-spring-damper system and an electron cloud can be used to describe resonance in metamaterials. In this analogy (Fig. 2.1) an electron cloud around the atom nucleus gets stretched with the application of an electric field *E* creating a local dipole defined by an electric displacement field *D*. When removing the electric field, just like the mass-spring-damper system, the electron cloud would move back and forth in an oscillatory pattern.

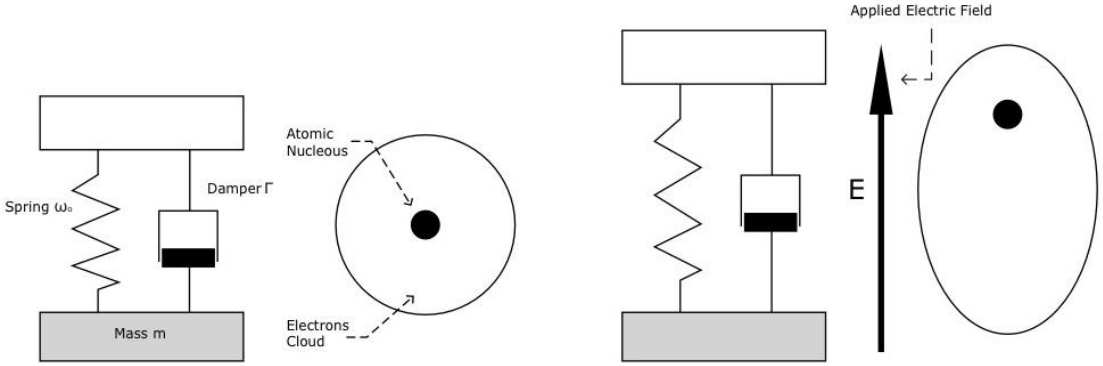

Figure 2.1. Comparison of a mass-spring system with the oscillation in atoms when an electric field is applied.

The system above, called *Lorentz Oscillator Model*, was proposed by Hendrik Lorentz [12] in an attempt to describe the interaction between atoms and electric fields in classical terms. The electron, which has a very small mass, is bound to the more massive nucleus of the atom, by a force that behaves according to Hooke's Law, i.e. a spring-like force. The applied electric field interacts with the charge of the electron, causing "stretching" or "compression" of the spring, which sets the electron into oscillating motion.

From the classical equation of motion (Eq. 2.1), and using complex mathematical transformations, it is possible to derive a dielectric function for the local electric dipole created (Eq. 2.2). This function will be written in terms of the *Lorentz parameters* and the resonating frequency, allowing a description of atomic scale resonances with classical formulation [12].

$$m\frac{\partial^2\vec{r}}{\partial t^2} + m\Gamma\frac{\partial\vec{r}}{\partial t} + m{\omega_0}^2 = -q\vec{E}; \quad \text{where } \omega_0 = \sqrt{\frac{K}{m}} \tag{2.1}$$

$$\tilde{\varepsilon}_r(\omega) = 1 + \frac{{\omega_p}^2}{{\omega_0}^2 - \omega^2 - j\omega\Gamma} \tag{2.2}$$

In Eq. (2.1), the first term on the left side of the equation accounts for the acceleration force, the second for the frictional force due to the damping Γ, the third term for the restoring force due to the natural or resonating frequency ω_0, and the term on the right accounts for the electric force due to the electric field *E*. In Eq. (2.2), ω is the angular frequency of the time-varying electric field driving the oscillator, ε_r is the relative electric permittivity of the medium related to the displacement in this oscillatory system; and ω_p is the plasma frequency of the material, for which an explanation goes beyond the interest of this document.

Because the electric permittivity was written in terms of angular frequency, this can be treated as a complex function, since complex numbers allow specification of magnitude and phase [13]. The real part of the permittivity is related to the stored energy within the medium, while the imaginary part is related to the loss of energy within the medium, hence, if the permittivity is zero, it means there is no energy dissipation. Therefore, it can be said that the imaginary part only exists when there is energy loss and in this case there will also be a contribution of the real part to the dissipation.

When plotting the real and imaginary parts of the permittivity separately, the result obtained presents the shapes seen in Fig. (2.2), which are typical of a Lorentz Model and are sometimes referred as *Lorentzian Functions* [12].

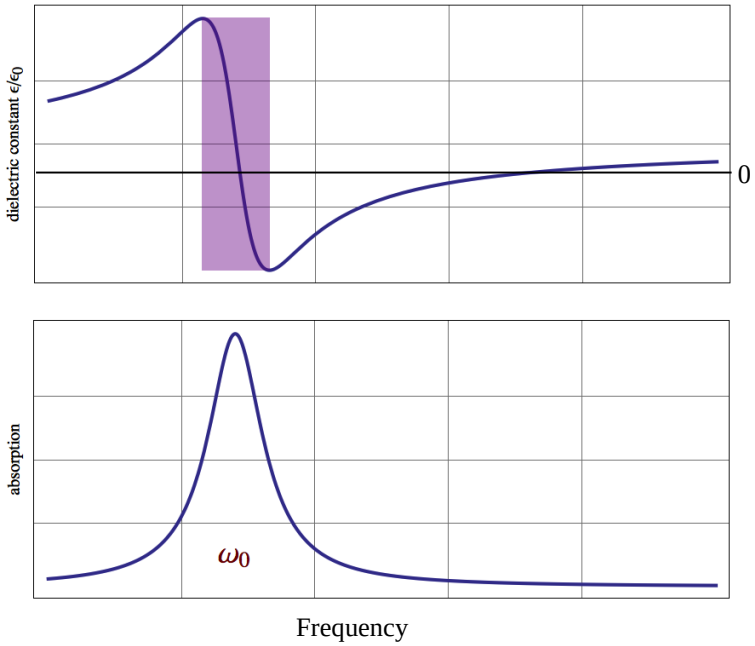

Figure 2.2. Real (top) and imaginary parts of the dielectric constant plotted as a function of the frequency.

One important aspect seen in Fig. (2.2) is that around the resonant frequency the dielectric constant suffers a considerable drop and presents negative values. This behaviour is not found in nature, where the permittivity can only be found with positive values, and is only possible to be obtained by the use of metamaterials.

Figure 2.2 shows that resonant metamaterials are absorptive around the resonance frequency. This property can introduce problems when considering light propagation, but is a vital characteristic for the sound attenuation of the acoustic metamaterials studied in this paper.

2.1 Resonant Acoustic Metamaterials

The physics and the formulation behind resonant acoustic metamaterials are similar to their electromagnetic analogue, with the difference that mechanical waves need a medium to transmit the energy. In such a medium, a bulk of material larger than the atomic scale yet smaller than the wavelength, can be defined as an acoustic particle [14] [15]. In this scenario, the two physical quantities that describe the wave are the dynamic pressure P of the medium and the velocity of the acoustic particles v, which have their relationship given by Eq. (2.3) below, where K is the bulk modulus or compressibility of the medium:

$$\nabla \cdot v = -K \frac{\partial P}{\partial t} \tag{2.3}$$

The acoustic particles oscillate in the medium, in the same way as the electron cloud of atoms of a dielectric material when an electric field is induced, as seen in Fig. (2.1). Hence, acoustic waves can also be analysed as a mass-spring-damper system and can be solved using the Lorentz Model. But in the acoustic environment, rather than electric permittivity, it will be the bulk modulus K to be written in terms of Lorentz parameters [16] [17] [18]:

$$\tilde{K}_{\mathrm{r}}^{-1}(\omega) = K_0^{-1}\left[1 - \frac{F\omega_0^2}{\omega^2 - \omega_0^2 - i\omega\Gamma}\right] \tag{2.4}$$

The geometric factor F in Eq. (2.4) is a comparison between the volume and the neck of the resonator, related to their capacity to scatter the sound waves inside the cavity [11]. In Eq. (2.4) above, ω_0 is the resonant angular frequency. As this is still a Lorentzian function, it is possible to separate and plot the real and imaginary parts of Eq. (2.4).

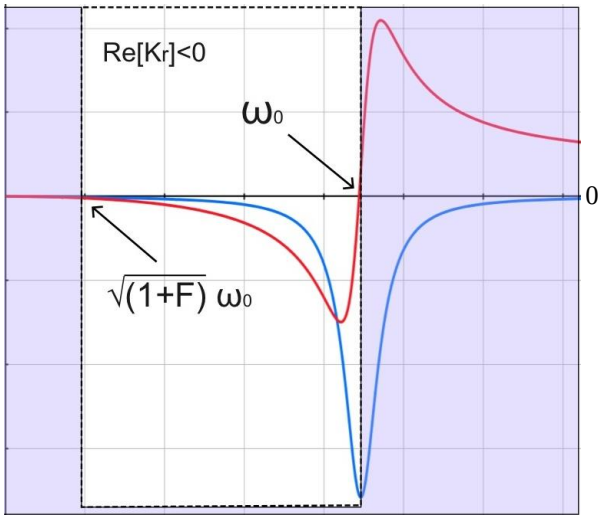

Figure 2.3. The real (red) and imaginary (blue) parts of the bulk modulus in a Lorentz Model.

Figure 2.3 shows that it is also possible to obtain negative values for the bulk modulus ($K < 0$). Previous experiments showed that it is possible to obtain metamaterials with a negative bulk modulus by concatenating Helmholtz resonators of sub-wavelength dimensions with a sub-wavelength periodicity [16] [19]. This can only happen in a specific frequency band, which is related to the resonant frequency of the resonators.

As mentioned previously, absorption occurs in the region where the imaginary part of the Lorentz function has values away from the zero limit. Figure 2.3 demonstrates that this will happen between the resonant frequency ω_0 and the frequency in which the real part of the bulk modulus becomes positive again as the frequency increases. In other words it can be understood that sound absorption will occur when the bulk modulus presents negative values.

At the cut-off frequency where the bulk modulus becomes positive again the loss is very low, and the damping factor can be considered to be zero [11]. With this information, it is possible to solve Eq. (2.4) to find the limiting frequency $\omega_{\text{CUT-OFF}}$, where the bulk modulus becomes positive (Fig. 2.3):

$$\omega_{\text{CUT-OFF}} = \sqrt{1+F}\,\omega_0 \tag{2.5}$$

Hence, it is possible to define that a negative bulk modulus will occur in an interval as the one shown in Fig. (2.3): $\omega_0 < \omega < \sqrt{1+F}\,\omega_0$. In this interval the negative bulk modulus is responsible for the separation of sound from its medium resulting in sound attenuation [11]. The Helmholtz resonators studied in this project were designed to present a negative bulk modulus respecting the conditions above (Eq. 2.4 and Eq. 2.5).

3. Resonators Design

In the material designed for this study (Fig. 3.1) each of the resonator cells was built individually with 5mm thick transparent acrylic and arranged in a specific matrix to form the metamaterial. Three kinds of individual resonator, also called *resonator cells* were built (Fig. 3.1), each with different internal volumes, in order to achieve attenuation over different frequency ranges. The first kind of resonator had one internal chamber with dimensions *150mm x 150mm x 40mm*. The second had two internal chambers of dimensions *150mm x 75mm x 40mm* and the third had four internal chambers, each with dimensions *75mm x 75mm x 40mm*.

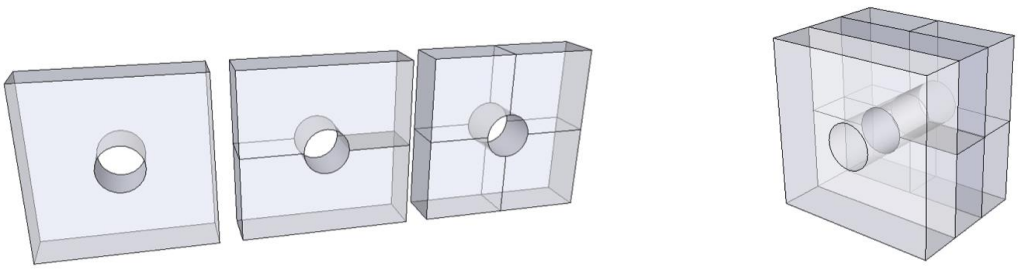

Figure 3.1. The three kinds of resonator cells built with one, two and four resonating chambers, respectively (left). The three kinds of resonator cells arranged in series (right).

Orifices with a diameter of *20mm* were made on each of the largest surfaces of the resonator cells. The orifices constitute the neck of the resonator cells and also allow air to flow through the sample. Diffraction at the orifice makes the sound waves diffuse inside the resonators and for this to happen, the diameter of the orifice must be smaller than the wavelength of the sound wave f [11]. Hence, the condition is that the frequencies need to be lower than the cut-off frequency f_{D}, for which the wavelength is the same as the size of the orifice: $f < f_{\text{D}}$.

The resonator cells were arranged in series (Fig. 3.1) to obtain a negative bulk modulus effect. Finally, to make the attenuation noticeable and to enhance the airflow effect, a panel sample (or window) of resonator cells was built with twelve three-layer sets in a *4 x 3* arrangement (Fig. 3.2). This construction replicates the design proposed by researchers at Mokpo National Maritime University [11].

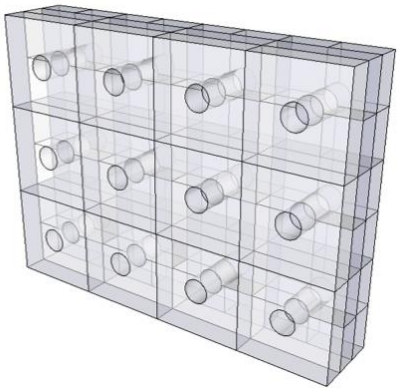

Figure 3.2. The final panel (or window) constituted of the different kinds of resonator cells.

3.1 Insertion Loss Measurements

A acoustic enclosure was built using *36mm* thick sheets of Medium Density Fibreboard (MDF) with dimensions *1.12* x *0.96* x *0.8m* (ratio *1:1.2:1.4*) to minimise internal modes in the frequency range of interest.

The acoustic enclosure was placed in the centre of an anechoic chamber with an omni-directional sound source (hemi dodecahedron) inside emitting pink noise. Two Class-1 sound level meters (SLMs) were placed 1.5m away from the sound source, 1m from the grid floor and at a 30º angle from each other (Fig. 3.3). Linear sound pressure levels L_Z between 500Hz-5kHz were measured in one-third-octave bands for this configuration.

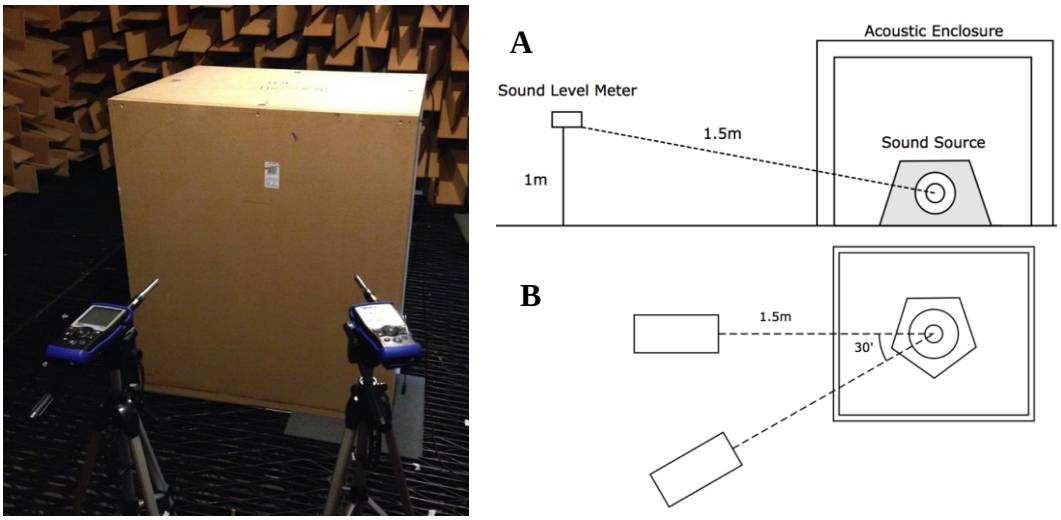

Figure 3.3 Insertion loss measurements with the acoustic enclosure. (A) Side View. (B) Top view.

Subsequently, an opening was cut in one of the enclosure's walls to accommodate the panel sample constituted of resonating cells. The acoustic enclosure, now with the window applied to it, was placed in the centre of the anechoic chamber with the sound source inside of it maintaining previous measurements conditions (Fig. 3.4). New L_Z levels between 500-5kHz were measured in this configuration for a comparison with the performance of the enclosure without the sample window.

Figure 3.5 presents the measured insertion loss levels for the acoustic enclosure with and without the window sample incorporated to it. Overall, the sound attenuation performance in the frequency region of interest (500Hz – 5kHz) of the acoustic enclosure increased by 3dB with the panel of resonators in place.

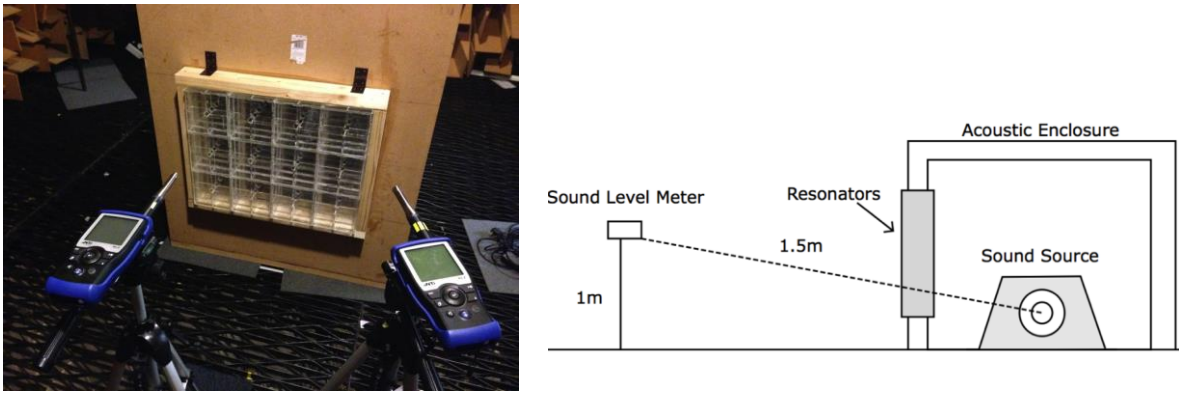

Figure 3.4 Insertion loss measurements with the sample applied to the acoustic enclosure.

At most frequencies in the region of interest, the performance of the enclosure with the window was the same or higher than that of the full enclosure with no resonators. Clear sound attenuation peaks can be observed at around 800Hz, 2kHz and 4kHz.

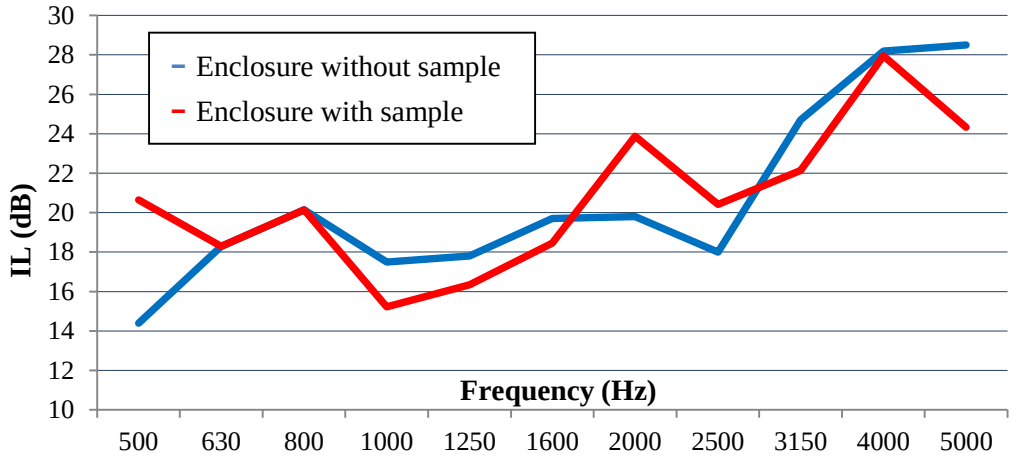

Figure 3.5 Insertion loss levels for the acoustic enclosure with and without sample.

Intuitively it would be expected that the insertion loss should be lower with the presence of a perforated window. However, the fact that the performance of this configuration was generally equal or better than that of the enclosure without the window sample is a clear indication that the negative bulk modulus of the sample is playing an important role in the sound attenuation performance.

Further work would include configuration modifications aiming to obtain higher IL levels over a broader frequency range, while allowing higher airflow rates. These would include air filters being applied to the neck of the resonators in order to make the attenuation peaks wider. Furthermore, different construction materials and arrangements involving different dimensions combinations could be investigated leading to sound attenuation over other frequency ranges.

4. Air Flow Resistance Tests

As mentioned previously, the airflow properties of the sample could provide the necessary ventilation for operational temperatures inside the enclosure. In order to verify such ventilation, airflow resistance tests were undertaken using a calibrated air flow test rig. The volume flow rate Q was determined with and without the enclosure applied to the rig for a range of different incident air velocities (Fig. 4.1).

The results presented in Fig. 4.2 below demonstrate that for low incident air velocities (approximately 7m/s) the airflow rate through the sample becomes very similar to the case where no enclosure is in place. This indicates that in a real case scenario where air velocities are at or lower than 7m/s, the sample would provide a considerable amount of ventilation to the enclosure.

A further assessment can be made by considering values of pressure loss factor due to the presence of the enclosure with the sample. The pressure loss due to the presence of the enclosure on the test rig was derived using an anemometer (Fig. 4.1) from which a Pressure Loss Factor ζ can be obtained.

Perforated sheets with a 20% free area ratio when applied to ventilation ducts are known to cause a pressure loss of $\zeta = 51$ [20]. The window sample applied to the enclosure has only 2% free area ration and its pressure loss factor was measured as being approximately 35, suggesting the pressure loss performance of the sample is comparable to that of perforated panels in ventilation ducts.

Figure 4.1 Air flow test rig with the enclosure with resonators and adaptor applied to it.

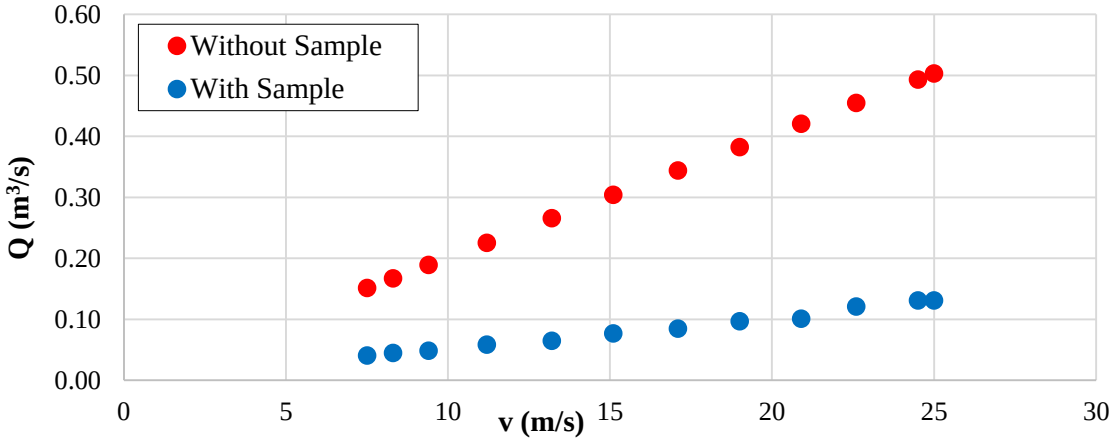

Figure 4.2 Volume flow rate vs incident air velocity with and without enclosure

5. Conclusions

The metamaterial construction investigated in this work applied to part of an acoustic enclosure showed clear indications of significant levels of sound attenuation over a wide frequency range. Airflow resistance tests demonstrated that the metamaterial sample tested does not restrict air flow significantly at the low air speeds typical of ventilated enclosed machinery.

These results demonstrate that it is possible to apply this kind of metamaterial to an acoustic enclosure and obtain favourable insertion loss in the frequency range of interest, while allowing suitable ventilation for the enclosure machinery.

REFERENCES

1 Smith, D. R., Padilla, W. J., Vier, D. C., Nemat-Nasser, S. C., Schultz, S. (2000) *Composite Medium with Simultaneously Negative Permeability and Permittivity*. Physical Review Letters 84 (18): 4184–7.

2 Engheta N. and Ziolkowski R. W. (2006) Metamaterials Physics and Engineering Explorations. New Jersey, USA: John Wiley & Sons, Inc

3 Ding Y., Liu Z., Qiu C., Shi J. (2007) *Metamaterial with Simultaneously Negative Bulk Modulus and Mass Density*. Phys. Rev. Lett. 99, 093904 (30th August 2007).

4 Liu, Z., Zhang, X., Mao, Y., Zhu, Y. Y., Yang, Z., Chan, C. T. and Sheng, P. (2000) *Locally Resonant Sonic Materials*. Science 289, 1734.

5 Li, J. and Chan, C. T. (2004) *Double-negative acoustic metamaterial*. Physical Review E, 70(5):055602(R), 2004.

6 Lee, S. H., Park, C. M., Seo, Y. M., Wang, Z. G. and Kim, C. K. (2009) *Acoustic metamaterial with negative density*. Physics Letters A, 373(17):4464, 2009.

7 Huang, H. H. and Sun, C. T. (2009) Wave attenuation mechanism in an acoustic metamaterial with negative effective mass density. New Journal of Physics 11 (2009) 013003 (15pp)

8 Zhang, S., Yin, L. and Fang, N. (no date) *Focusing Ultrasound with Acoustic Metamaterial Network.* [Online]. Available from: http://arxiv.org/pdf/0903.5101.pdf [Accessed on 20th October 2014].

9 Zhang, S., Xia, C. and Fang, N. (no date) *Broadband Acoustic Cloak for Ultrasound Waves*. [Online]. Available from: http://arxiv.org/pdf/1009.3310.pdf [Accessed on 20th October 2014].

10 Mei, J., Ma, G., Yang, M., Yang, Z., Wen, W. and Sheng, P. (2012) *Dark acoustic metamaterials as super absorbers for low-frequency sound*. Nature Communications, DOI: 10.1038/ncomms1758.

11 Kim, S. H. and Lee, S. H. (2013) *Air Transparent Soundproof Window*. [Online]. Available from: http://arxiv.org/abs/1307.0301. [Accessed on 15th April 2014].

12 Almog, I.F., Bradley, M.S. and Bulovic, V. (2011) *The Lorentz Oscillator and its Applications*. MIT OpenCourseWare. [Online]. Available from: ocw.mit.edu [Accessed on 11th October 2014].

13 Purcell, E. M. (1985) *Electricity and Magnetism Berkeley Physics Course Volume 2*. 2nd Edition. Berkeley, USA: McGraw-Hill.

14 Zigoneanu, L. (2013) *Design and Experimental Applications of Acoustic Metamaterials*. PhD dissertation. Durham, USA: Duke University.

15 Zang, S. (2010) *Acoustic Metamaterial Design and Applications*. PhD dissertation. Urbana, USA: University of Illinois.

16 Fang, N., Xi, D. J., Xu, J. Y., Ambati, M., Srituravanich, W., Sun, C. and Zhang, X. (2006) *Ultrasonic metamaterials with negative modulus*. Nature Materials, 5(6):452– 456, 2006.

17 Lee, S. H., Park, C. M., Seo, Y. M., Wang, Z. G. and Kim, C. K. (2009) *Acoustic metamaterial with negative density*. Physics Letters A, 373(17):4464, 2009.

18 Huang, H. H. and Sun, C. T. (2009) *Wave attenuation mechanism in an acoustic metamaterial with negative effective mass density*. New Journal of Physics 11 (2009) 013003 (15pp)

19 Mahesh N. R. and Prita, N. (2011) *Experimental and Theoretical Investigation of Acoustic Metamaterial With Negative Bulk-Modulus*, in: COMSOL Conference, Bangalore. [Online]. Available from: http://www.comsol.com/paper/download/84127/mahesh_paper.pdf [Accessed on 19th October 2014].

20 Chartered Institution of Building Services Engineers *CIBSE Guide B: Heating, Ventilating, Air Conditioning & Refrigeration*. London, CIBSE: 2001.